

# NUMERICAL SIMULATION OF CONTAMINANT REMOVAL DURING AIR SPARGING

Nenad JACIMOVIC<sup>1</sup>, Takashi HOSODA<sup>2</sup>, Kiyoshi KISHIDA<sup>3</sup> and Marko IVETIC<sup>4</sup>

<sup>1</sup>PhD Student, Department of Urban Management, Kyoto University

<sup>2</sup>Member of JSCE, Professor, Department of Urban Management, Kyoto University

<sup>3</sup>Member of JSCE, Associate Professor, Department of Urban Management, Kyoto University

<sup>4</sup>Professor, Faculty of Civil Engineering, Belgrade University (Serbia)

The paper presents a mechanistic model for simulation of mass removal during air sparging. Model takes into account several processes which are commonly neglected, such as air channeling and advection by the water phase. Diffusion of contaminants towards the air channels is modeled as a first order kinetic between the two water compartments. The adopted model of contaminant evaporation at the air-water interface is verified by comparison with reported experimental results. Model is used for simulation of two-dimensional air sparging laboratory experiment conducted by Reddy and Tekola (2004). Good overall agreement is observed. It is showed that natural groundwater flow can influence the efficiency of the air sparging.

*Key Words: air sparging, multi-phase flow model, numerical simulation*

## 1. INTRODUCTION

The in-situ air sparging (IAS) is one of available technologies for removal of volatile organic compounds (VOCs) from groundwater<sup>1</sup>. The concept of remediation is relatively simple: air is injected into the saturated zone and contaminant removal is promoted through volatilization into the air plume and enhancement of biodegradation by increasing the dissolved oxygen in groundwater.

Optimal design of IAS system requires prediction of air distribution in the saturated zone as well as the rate of mass transfer into the air stream. Both quantities depend on soil properties, contaminant characteristics and operational parameters such as air injection flow rate. From the point of numerical modeling, there are two issues considering air sparging: modeling of air flow and distribution and modeling of mass transport and transfer.

A number of researchers have studied air sparging by the experimental observations on the laboratory<sup>2,3</sup> or in situ<sup>4</sup> scales. Reported results indicate that there are two air flow patterns, depending on average grain size of porous media: air flow through the network of discrete channels and bubbly flow pattern. Brooks et al.<sup>5</sup> summarized the published experimental observations and also conducted their own experiments with glass beads. They concluded that channel flow occurs in porous

media up to 1 to 2mm, and bubble flow in media greater than 1 to 2mm. According to the Unified Soil Classification System, this transition zone occurs in medium sand. As they admitted, identification of the air flow pattern is subjective in nature, and cannot always be clearly distinguished.

To date, several numerical models are published for simulation of air flow in saturated soils<sup>6,7</sup>. All of them are based on the multiphase theory with relative permeability concept. Chen et al, for example, showed that this approach produces very good predictions of air saturations<sup>8</sup>. They used X-ray computed tomography imaging to measure air content of the soil. However, hydraulic properties of the soil have to be very well characterized in order to apply a numerical model.

Mass transfer modeling during air sparging appears to be a more difficult task. There are generally two types of current models for simulation of mass removal<sup>9</sup>. First type represents mechanistic models based on multidimensional governing flow and transport equations. Second group make simplified, so called "reactor" models, where mass removal is related to the quantity of fluids circulating in the reactor zone. Models of McCray and Falta<sup>10</sup> and Unger et al.<sup>11</sup> are the mechanistic ones. In these models hydrodynamics and mass transport within each phase is simulated. However, both models assume instantaneous equilibrium between liquid and gas phase (Henry's law) which is

shown to give significantly “optimistic” results considering required time of remediation<sup>(12),13)</sup>.

Rabideau et al. (1999) proposed a “reactor” model which takes into account diffusion towards the air channels. They succeeded to reconstruct source zone tailing and rebound behavior, often observed at the air sparging sites. In this model the sparging region is modeled as a reactor consisting of two mixed compartments, where only one of these compartments exchange mass with the air phase. Model, however, does not include transport of contaminants by the air phase and advection by the water phase.

Similar model is proposed by Elder et al. (1999). This model considers air flow in discrete air channels, diffusion between the air channels and rate limited mass transfer into the air phase. Water phase is assumed as stationary and sorption is neglected. Air phase distribution is assumed in this model, based on air injection flow rate. Therefore, it is not clear how to model nonhomogeneous porous media, or how to model several sparging wells with overlapping radius of influence.

In this paper, a numerical model is presented which considers all of aforementioned properties relevant for mass transfer during the air sparging. Model includes hydrodynamics of air and water phase. Calculated air volume content is divided into a number of air channels surrounded by the water phase, which is divided into two compartments. First compartment is immobile and it is in contact with air phase, while the second compartment is mobile. This “mobile-immobile” formulation is a common approach for description of solute transport by groundwater. Mass transfer between two water compartments is modeled as a first order kinetic, where the mass transfer coefficient, representing diffusion and advection in the water phase towards the air channels, is parameter needed to be calibrated. Sorption for both water compartments is considered.

## 2. MODEL FORMULATION

### (1) Two-phase flow model

Prior to mass transport/transfer calculation, at the each time step air and water flow fields have to be obtained. Here, the two-phase model described in Jacimovic et al. (2006) is used. Governing equations for laminar, two phase (air and water) flow of incompressible fluids in rigid porous media are as follows:

$$\frac{\partial \theta_p}{\partial t} + \frac{\partial}{\partial x_i} (\theta_p U_{pi}) = 0, \quad p = a, w \quad (1)$$

$$\rho_p \theta_p \frac{\partial U_{pi}}{\partial t} + \rho_p \theta_p U_{pi} \frac{\partial U_{pi}}{\partial x_j} = \rho_p \theta_p g_i - \theta_p \frac{\partial p_p}{\partial x_i} + \frac{\partial}{\partial x_j} \left( \theta_p \mu_p \frac{\partial U_{pi}}{\partial x_j} \right) - \lambda_p \theta_p^2 U_{pi} \quad (2)$$

$$\theta_a + \theta_w = \phi, \quad (3)$$

where  $\rho_p$  is the  $p$ -phase density ( $M/L^3$ ),  $\theta_p$  is the volumetric content of the phase ‘ $p$ ’ ( $L^3/L^3$ ),  $\mu_p$  is the fluid viscosity ( $M/LT$ ),  $g_i$  the gravitational acceleration ( $M/T^2$ ),  $U_{pi}$  the pore velocity of the phase ‘ $p$ ’ ( $L/T$ ),  $p_p$  the phase pressure ( $M/LT^2$ ) and  $\phi$  is the “effective” porosity (dimensionless). Subscription ‘ $p$ ’ denotes phase (‘ $a$ ’ for the air and ‘ $w$ ’ for the water). The last term in equation (2) represents the drag term comprising the influence of porous media and presence of another fluid through the parameter  $\lambda_p$ , which is, according to relative permeability concept, defined as:

$$\lambda_p = \frac{\mu_p}{k k_{rp}}, \quad (4)$$

where  $k$  is the intrinsic permeability of the porous media ( $L^2$ ), and  $k_{rp}$  is the relative permeability (dimensionless). The phase content can also be expressed as saturation ( $S_p$ ) by relation  $S_p = \theta_p / \phi$ .

Model includes acceleration terms in momentum equations, since in some cases it can be significant, as discussed by Jacimovic et al. (2006).

### (2) Mass transport model

The mechanisms affecting volatile contaminant removal during air sparging include: air advection, air diffusion, volatilization, water advection, water diffusion/dispersion, sorption and chemical/biological reactions. Depending on the soil and contaminant properties, some of these processes can be more or less significant.

We assume that a continuous film of water, which is the wetting fluid, coats the soil grains so that mass transfer between soil and air is possible only via the water phase. Water phase is divided into two compartments, which coincide with “clear” and “dirty” zones in the conceptual model of Rabideau et al. (1999). The immobile water compartment is in contact with the air phase, while the mobile water compartment is not. Partitioning between water and soil is assumed as an instantaneous equilibrium.

The mass conservation equations for the air, immobile water and mobile water phase in Cartesian coordinates are:

$$\frac{\partial (\theta_a C_a)}{\partial t} = - \frac{\partial (C_a \theta_a U_a)}{\partial x_i} + \theta_a K_{wa} A (HC_{wi} - C_a), \quad (5)$$

$$\frac{\partial(\theta_{wi}C_{wi})}{\partial t} = -\theta_a K_{wa} A (HC_{wi} - C_a) + \theta_{wi} K (C_w - C_{wi}) - \rho_b f K_d \frac{\partial C_{wi}}{\partial t}, \quad (6)$$

$$\frac{\partial(\theta_w C_w)}{\partial t} = -\frac{\partial(C_w \theta_w U_{wi})}{\partial x_i} + \theta_w D_w \frac{\partial^2 C_w}{\partial x_i^2} - \theta_{wi} K (C_w - C_{wi}) - \rho_b (1-f) K_d \frac{\partial C_w}{\partial t}, \quad (7)$$

where  $C_a$ ,  $C_{wi}$  and  $C_w$  are the air, immobile water and mobile water concentrations ( $M/L^3$ ),  $\theta_{wi}$  is the immobile water volume content,  $K_{wa}$  is the air-water mass transfer coefficient ( $L/T$ ),  $A$  is the contact surface between air and water phase per unit volume of porous media ( $L^2/L^3$ ),  $H$  is the Henry's constant (dimensionless),  $K$  is the immobile-mobile water transfer coefficient ( $T^{-1}$ ),  $\rho_b$  is the soil dry bulk density ( $M/L^3$ ),  $f$  is the fraction of sorbent associated with immobile water compartment (dimensionless) and  $D_w$  is the water dispersion coefficients ( $L^2/T$ ).

The air-water mass transfer coefficient ( $K_{wa}$ ) is estimated in the same way as in the conceptual model of Elder et al. (1999). It is assumed that  $K_{wa}$  is a function of resistance of the air and liquid film at the interface. Considering water film as a stagnant, a penetration theory<sup>14</sup> can be applied for calculation of the water film resistance. In that case,  $K_{wa}$  can be expressed as:

$$K_{wa} = \left\{ \frac{d^{2/3} L^{1/3}}{1.615 D_a (Re Sc)^{1/3}} + \frac{d \pi H}{4} \left( \frac{L}{D_{wo} \alpha_a U_a} \right)^{1/2} \right\}^{-1} \quad (8)$$

where  $D_a$  and  $D_{wo}$  are the air and water diffusion coefficients ( $L^2/T$ ),  $d$  is the air channel diameter ( $L$ ),  $L$  is the air channel length ( $L$ ),  $Re$  and  $Sc$  are the Reynolds and Schmidt numbers, respectively. These nondimensional numbers are defined as:

$$Re = \frac{(\theta_a U_a) d}{\mu_a}, \quad (9)$$

$$Sc = \frac{\mu_a}{\rho_a D_a}. \quad (10)$$

The air-water interface area is estimated under assumption that air channels are evenly distributed in the horizontal plane of one calculation cell:

$$A = \frac{4\theta_a}{d\sqrt{\tau}}, \quad (11)$$

where  $\tau$  is the tortuosity of the air channels (dimensionless). Assuming a hexagonal pattern of air channel distribution, calculated interface area by Elder and Benson (1999) was in good agreement with earlier published results<sup>15</sup>.

Equilibrium partitioning between the dissolved and the solid phase (sorption) is modeled as a Freundlich isotherm:

$$C_s = K_d [fC_{wi} + (1-f)C_w], \quad (12)$$

where  $C_s$  is the soil concentration ( $M/M$ ),  $K_d$  is the distribution coefficient ( $L^3/M$ ), usually expressed as a product of mass fraction of organic carbon in the soil and organic carbon partitioning coefficient ( $K_d = f_{oc} K_{oc}$ ). It is assumed that sorbent is uniformly distributed between immobile and mobile water, resulting that fraction of sorbent associated with immobile water can be calculated as  $f = \theta_{wi} / (\theta_{wi} + \theta_w)$ .

In the presented model, the immobile water content is taken as constant and equal to the residual water content.

### 3. VALIDATION OF THE AIR-WATER MASS TRANSFER ESTIMATE

There are two important parameters in the model: air-water mass transfer ( $K_{wa}$ ) and mobile-immobile water mass transfer ( $K$ ). Generally, the air-water interface area ( $A$ ) can not be experimentally determined. Therefore, it is a common practice to measure the lumped value of mass transfer ( $K_{wa}A$ ). As stated earlier, the same approach for  $K_{wa}A$  modeling is used in the conceptual model of Elder et al. (1999), however, no explicit validation of equations (8) and (11) is published in the literature yet. That was the main motive of the study described in this section.

In order to test adopted method for estimation of air-water mass transfer, it will be applied on published experimental results. Chao et al. (1998) reported one-dimensional experiments in order to investigate air-water mass transfer of VOCs<sup>16</sup>. Their experimental setup consisted of a Plexiglas column, 9.5cm in diameter and 40.6 cm in height, in which the clean soil was placed. The soil was then saturated with contaminated water, sealed and allowed to equilibrate before air injection. Air was injected into the bottom of the column and concentration of VOCs in the effluent air was measured periodically. From the simple mathematical model, the best fitting values of the air-water mass transfer were reported. For model validation in this study, the experiments with coarse sand are used.

The one-dimensional numerical model is used to calculate a steady air saturation for a given air injection flow rate. The hydraulic permeability and porosity of the soil are reported by the authors, however, parameters of capillary pressure and relative permeability curves are calibrated from the reported values of total volume of air channels for a given air flow rate. For example, in the case of

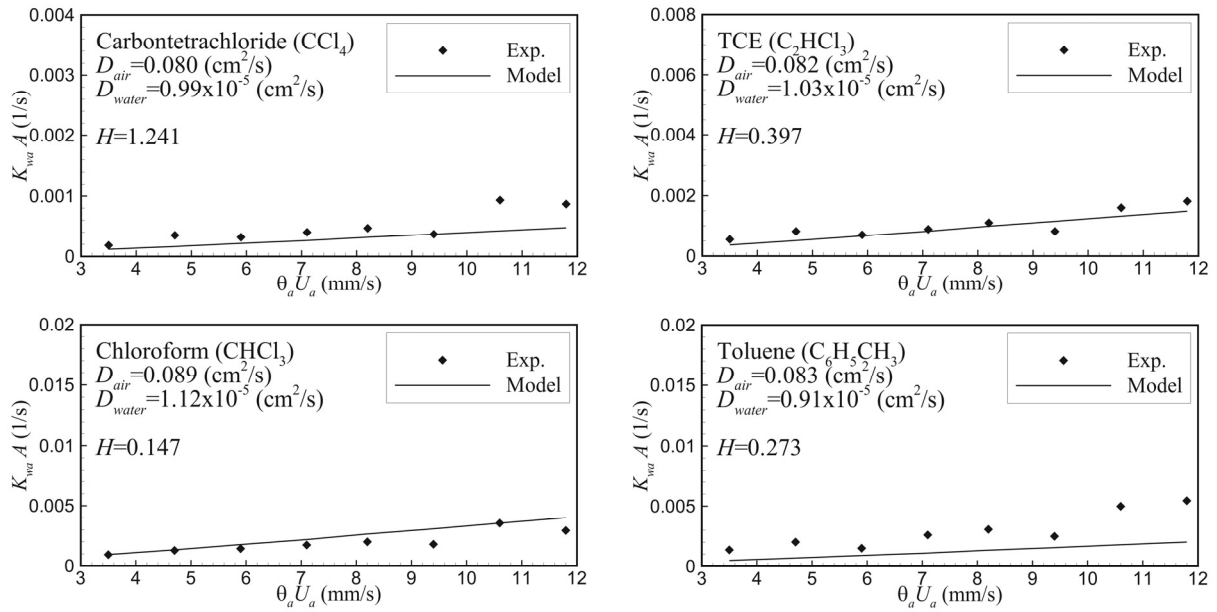


**Fig. 1.** Comparison of calculated (lines) and measured (dots) values of lumped air-water mass transfer coefficients

coarse sand, at the air flow rate of 5.0 L/min, reported total volume of the air channels was 0.089L.

For capillary pressure and relative permeability curves, van Genuchten model is utilized:

$$p_c = \frac{\rho_w g}{\alpha_{aw}} (S_w^{-1/m} - 1)^{1/n}, \quad (13)$$

$$k_{rw} = S_w^{1/2} \left\{ 1 - \left( 1 - S_w^{1/m} \right)^m \right\}^2, \quad (14)$$

$$k_{ra} = (1 - S_w)^{1/2} \left( 1 - S_w^{1/m} \right)^{2m}, \quad (15)$$

where  $p_c = p_a - p_w$  is the capillary pressure,  $m = 1 - 1/n$  and  $\alpha_{aw}$  are the fitting parameters. Used parameter values are shown in Table 1.

Assuming the average value of the air channel diameter from the reported values in the literature, the air-water interface area is calculated from equation (11) and transfer coefficient from equation (8). Figure 1 shows comparison between calculated and measured values of lumped mass transfer coefficients as a function of air Darcy-velocities for several VOCs. Considering complexity of the process and a number of approximations adopted, a good overall agreement is achieved. Sensitivity analysis showed that air channel diameter has the greatest influence on obtained results. In the experimental work of Elder and Benson (1999), reported air channel diameters for several types of the soil were between 1mm and 11.5mm. In the absence of more reliable information, it can be recommended to use a higher values, in which case the error is conservative.

**Table 1.** Soil parameters used for calculation of air-water mass transfer

Parameter	Value
Hydraulic permeability	$5.49 \times 10^{-4}$ [m/s]
Porosity	0.41 [-]
Residual water content	0.06 [-]
$\alpha$ parameter in eq. (13)	10.0 [1/m]
$n$ parameter in eqs. (13) - (15)	1.2 [-]
Soil column length	0.305 [m]
Air channel diameter	0.01 [m]
Air channel tortuosity	0.9 [-]
Organic carbon content ( $f_{oc}$ )	0.3 [%]

#### 4. APPLICATION TO 2D AIR SPARGING EXPERIMENT

Presented model is verified by the application on 2D air-sparging experiments reported by Reddy and Tekola<sup>17)</sup>. Their 2D apparatus consisted of 111cm x 72cm x 10cm Plexiglas tank which was divided into 3 compartments. The middle compartment was soil chamber, 91cm in length. Two other compartments, each measuring 10 cm in length, were placed on two sides of the middle one, representing reservoirs with fixed water level (Figure 2). By changing the water level in the reservoirs, natural groundwater flow can be simulated in the soil chamber.

Uniform coarse sand with hydraulic permeability of 0.05 cm/s and porosity 0.4 was used. As VOC contaminant, trichloroethylene (TCE) solution was prepared and injected into the soil profile prior the air sparging. During the air sparging course, a TCE concentration was measured in the sampling points (SP) showed in Fig. 2.

The numerical grid consists of elements that represent one-inch squares. Constant atmospheric gas pressure is maintained at the top boundary and

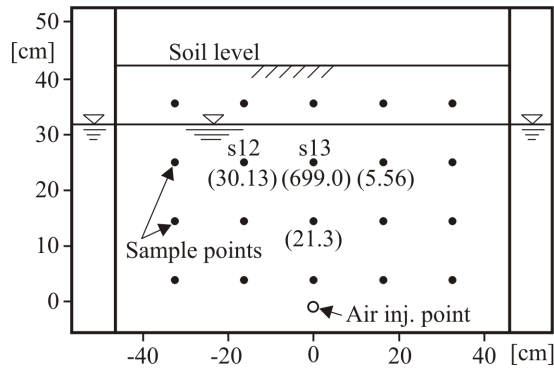


**Fig. 2.** Laboratory setup for air sparging simulation. Values in brackets represent initial TCE concentrations (mg/L) for air sparging simulation (Reddy and Tekola, 2004).

**Table 2.** Soil parameters adopted for simulation

Parameter	Value
Residual water content	0.06 [-]
$\alpha$ parameter in eq. (13)	9.0 [1/m]
$n$ parameter in eqs. (13) - (15)	3.2 [-]
Soil column length	0.305 [m]
Air channel tortuosity	0.9 [-]
Longitudinal dispersivity	0.01 [m]
Transverse dispersivity	0.001 [m]
Organic carbon content ( $f_{oc}$ )	0.1 [%]

hydrostatic pressure is imposed at the side walls of the soil chamber. The initial condition for air sparging simulation is obtained by imposing prescribed water level and running the simulation until the equilibrium between gravity and capillary forces is reached. The soil parameters, which are not reported by the authors are assumed as typical for the sand soil (Table 2). Characteristics of a TCE contaminant are taken the same as in the previous section.

The only calibrated parameter is the mobile-immobile water transfer coefficient ( $K$ ). This parameter represents diffusion and advection of the contaminants towards the air channels. Since the representative diffusion length depends on the number of air channels, i.e. the distance between them, the  $K$  coefficient must depend on the air saturation. Approximating the  $K$  as a inversely proportional to the square of channel distance (Rabideau et al., 1999) and the air channels as uniformly distributed in the horizontal plane of calculation cell, it can be easily shown that  $K$  is proportional to the air phase content. Therefore, we propose a following dependence for the coefficient  $K$ :

$$K = K_0 \left( 1 + \frac{\alpha_a}{\alpha_{a0}} \right) \quad (16)$$

where  $K_0$  is a mass transfer coefficient, calibrated at the referent air phase content ( $\alpha_{a0}$ ) for specific soil.

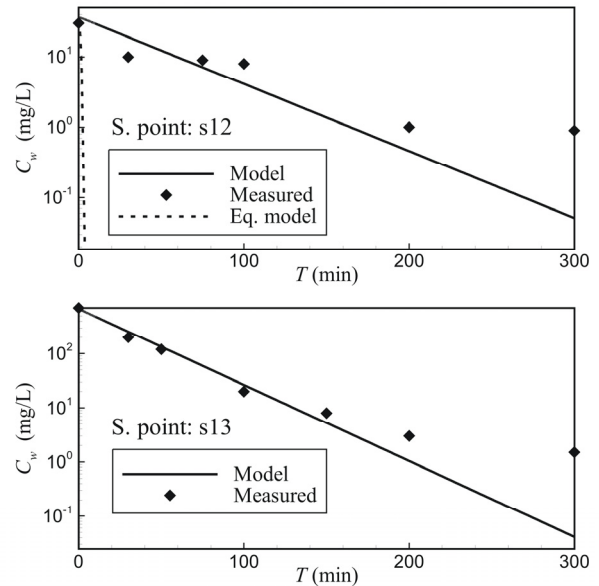


**Fig. 3.** Comparison of calculated and measured TCE concentrations: a) Sampling point 's12', b) Sampling point 's13'.

### (1) Simulation with static groundwater condition

First, model is applied to the case of static groundwater condition. Figure 2 shows SP initial concentrations (Reddy and Tekola, 2004). In this study, an air injection rate of 7.125 L/min is simulated. Calibrated value of mobile-immobile transfer coefficient is estimated as  $K_0 = 2.1 \times 10^{-4}$  1/s at the air phase content of  $\theta_{a0} = 0.11$ .

Comparison of simulated and measured TCE concentrations at SP 's12' and 's13' is showed in Fig. 3. As it can be seen in Figure 3-b), the agreement of simulated concentrations at the point 's13' is very good. At the SP 's12', however, there is some discrepancy, but overall agreement is still very well. There are two possible reasons for this discrepancy: (1) values of initial concentrations between sampling points are linearly interpolated, which probably was not the real case; (2) initial concentrations between sampling points and the free surface is unknown and it is possible that density driven flow occurred which caused almost constant concentration in the period between 20 and 100 min. after start of air sparging.

As a comparison, the same scenario is simulated with instant equilibrium assumption between air and the water phase (Eq. model). Results for the SP 's12' are showed in Fig. 3-a). At the SP 's13' the mass removal is even faster because of higher air saturation.

### (2) Simulation with groundwater flow

As illustration of the groundwater flow effect on air sparging performance, two simulations are conducted with different air injection flow rates. Initial conditions, as well as computational

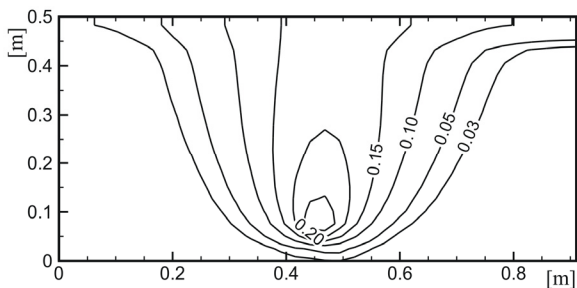


**Fig. 4.** Air saturation contours for air flow rate of 4.0L/min and water hydraulic gradient 0.03.

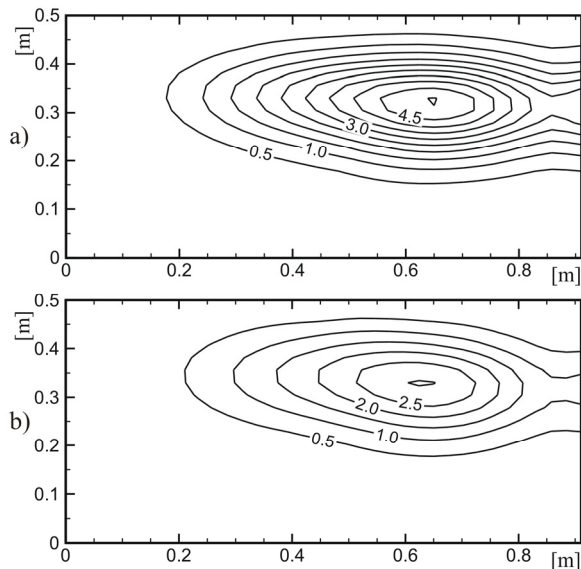


**Fig. 5.** Comparison of calculated TCE concentrations (mg/L) 2.5h after start of simulation: a) 1.5 L/min air injection rate, b) 4.0 L/min air injection rate.

parameters are the same as the previous case with stagnant groundwater. The only difference is the 0.03 hydraulic gradient, imposed by rising the water level of the left reservoir. Two air injection flow rates are simulated: 1.5 L/min and 4.0 L/min.

Air saturation contours for the case of 4.0L/min air flow rate is showed in Fig. 4. It is observed that water flow slightly affects air distribution, so it is not symmetric. Concentration distribution, 2.5 hours after start of air sparging, is showed in Fig. 5. It can be seen that some amount of contamination “escapes” the zone of influence of the sparging well. At the air flow rate of 1.5L/min the observed concentrations are about 70% higher than in the case of 4.0L/min air flow rate. It is clear that natural ground water flow has to be considered in the air sparging simulations.

## 5. CONCLUSIONS

A new, mechanistic model for simulation of mass transfer/transport during air sparging has been developed. Application to reported experiments showed capability of the presented model to

simulate observed contaminant removal. It was confirmed that equilibrium assumption is inadequate for air sparging simulations. It is also shown that natural groundwater flow has to be considered during the design of optimal air sparging system.

## REFERENCES

- 1) Johnson, R.L., P.C. Johnson, D.B. McWhorter, R.E. Hinchee, and I. Goodman, An overview of in situ air sparging, *Ground Water Monit. Rem.*, 13 (4), pp. 127-135, 1993.
- 2) Ji, W., A. Dahmani, D.P. Ahlfeld, J.D. Lin, and E. Hill, Laboratory study of air sparging: Air flow visualization, *Ground Water Monit. Rem.*, 13 (4), pp. 115-126, 1993.
- 3) Semer, R., J.A. Adams and K.R. Reddy, An experimental investigation of air flow patterns in saturated soils during air sparging, *Geotech. Geol. Eng.*, 16, pp. 59-75, 1998.
- 4) Lundegard, P.D. and D. LaBrecque, Air sparging in a sandy aquifer: Actual versus apparent radius of influence, *J. Contam. Hydrol.*, 19(1), pp. 1-27, 1995.
- 5) Brooks, M.C., W.R. Wise, and M.D. Annable, Fundamental changes in in situ air sparging flow patterns, *Ground Water Monit. Rem.*, 19 (2), pp. 105-113, 1999.
- 6) McCray, J.E. and R.W. Falta, Numerical simulation of air sparging for remediation of NAPL Contamination, *Ground Water*, 35 (1), pp. 99-110, 1997.
- 7) Jacimovic, N., T. Hosoda, K. Kishida and M. Ivetic, Two-phase numerical model for air sparging simulation with modeling of acceleration terms, *J. App. Mechanics*, JSCE, (9), pp. 765-771, 2006.
- 8) Chen M.R., R.E. Hinkley and J.E. Killough, Computed tomography imaging of air sparging in porous media, *Water Resour Res.*, 32(10), pp. 3013-3024, 1996.
- 9) Rabideau, A.J. and J.M. Blyden, Analytical model for contaminant Mass Removal by Air Sparging, *Ground Water Monit. Rev.*, Fall, pp. 120-130, 1998.
- 10) McCray, J.E. and R.W. Falta, Defining the air sparging radius of influence for groundwater remediation, *J. Contam. Hydrol.*, 24, pp. 25-52, 1996.
- 11) Unger, A., E. Sudicky and P. Forsyth, Mechanisms controlling vacuum extraction coupled with air sparging for remediation of heterogeneous formations contaminated with dense non-aqueous phase liquids, *Water Resour Res.*, 31, pp. 1913-1925, 1995.
- 12) Rabideau, A.J., J.M. Blyden and C. Ganguly, Field Performance of Air-Sparging System for Removing TCE from Groundwater, *Environ. Sci. Technol.*, 33(1), pp. 157-162, 1999.
- 13) Elder C.R., C.H. Benson and G.R. Eykholt, Modeling Mass Removal during In Situ Air Sparging, *Journal of Geotechnical and Geoenvironmental Eng.*, 125, pp. 947-958, 1999.
- 14) Bird, R., W. Stewart and E. Lightfoot, *Transport Phenomena*, Wiley New York, 1960.
- 15) Elder C.R. and C.H. Benson, Air Channel formation, Size, Spacing and Tortuosity During Air Sparging, *Ground Water Monit. Rev.*, Summer, pp. 171-181, 1999.
- 16) Chao K.P, S.K. Ong and A. Prototapas, Water-to-air Mass Transfer of VOCs: Laboratory-Scale Air Sparging System, *Journal of Environmental Engineering.*, November, pp. 1054-1060, 1998.
- 17) Reddy K.R. and L. Tekola, Remediation of DNAPL source zones in groundwater using air sparging, *Land Contamination and Reclamation*, 12(2), pp. 67-83, 2004.